engineering proceedings

MDPI

Proceeding Paper

Modeling and Simulation of Planar Transformer for Flyback Converter †

Hristo Ibrishimov [1], Dimitar Arnaudov [2] and Milko Yovchev [1,*]

[1] Department of Electric Power Distribution and Electrical Equipment, Technical University of Gabrovo, 5300 Gabrovo, Bulgaria; ico@tugab.bg
[2] Department of Power Electronics, Technical University of Sofia, 1000 Sofia, Bulgaria; dda@tu-sofia.bg
* Correspondence: myovchev@tugab.bg
† Presented at the 15th International Scientific Conference TechSys 2026—Engineering, Technologies and Systems, Plovdiv, Bulgaria, 14–16 May 2026.

Abstract

In this paper, the design of a planar transformer for a flyback converter and modeling using the finite element method are presented. Results are obtained for primary and secondary winding inductance, transformer leakage inductance, winding parasitic capacitances, winding current density, magnetic flux density, and distribution of magnetic field lines. A simulation of the operation of the converter in the continuous current mode and in border mode was made to validate the obtained electrical parameters.

Keywords: planar transformer; equivalent parameters; modeling of electromagnetic field

1. Introduction

The high-frequency transformer is a main component in galvanically isolated pulse converters, and the determination of its equivalent parameters is a major scientific and engineering task in their design [1,2]. The efficiency of pulse converters depends on the correct selection of the number of windings, the material and section of the magnetic wire, the current density, and other parameters of the high-frequency transformer.

The use of planar transformers in high-frequency pulse converters has been increasing in recent years, due to their undeniable advantages over traditional transformers, such as: compact dimensions; repeatability of parameters; easier to manufacture; lower price; smaller leakage inductance; better cooling; possibility to reduce the volume of the converter [3–6]. The main disadvantages of planar transformers are: large self-capacitance of the windings; reduced utilization factor of the core's window [7].

As a result of the non-linearity of the characteristics of the materials that construct the planar transformers, there are no universal analytical approaches for determining the equivalent parameters. This significantly complicates their design and prevents the development of universal solutions [8]. One possible approach is to use numerical methods to model the electromagnetic field of the transformer and numerically determine the equivalent and parasitic elements in the transformer.

The aim of this paper is to create a 3D model of a planar transformer for a flyback converter, to study using the finite element method the effect of the air gap on the inductance of the primary winding, to determine the magnetizing inductance, the leakage inductance, the self-capacitances of the windings and the active resistances.

Check for updates

Academic Editors: Nikola G. Shakev, Valyo N. Nikolov, Nikolay R. Kakanakov and Sevil A. Ahmed-Shieva

Published: 30 July 2026

Copyright: © 2026 by the authors. Licensee MDPI, Basel, Switzerland. This article is an open access article distributed under the terms and conditions of the Creative Commons Attribution (CC BY) license.

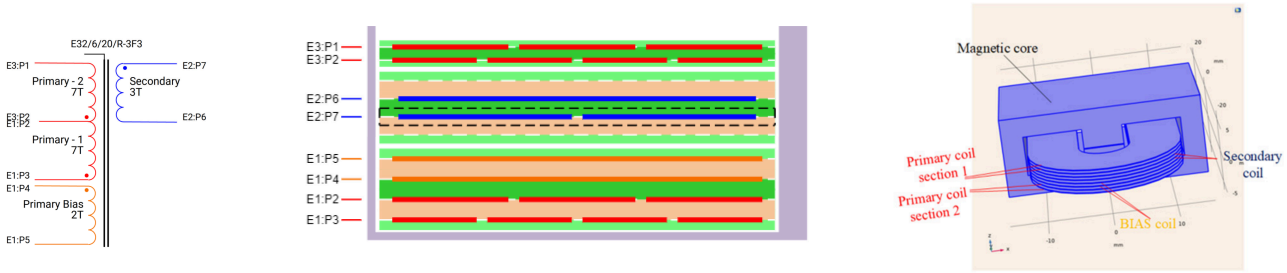
2. Description of the Model

The planar transformer, which is the object of the present modeling, is included in the composition of the flyback converter. A 3D model is used, which consists of the primary, secondary, bias coil and transformer's core. In advance, the design of the flyback converter and the planar transformer in the PI Expert software (ver. 2.9) environment has been done. The design results are shown in Table 1.

Table 1. Planar transformer design results.

Parameters	Value/Material
Minimum DC input voltage, V	234.9
Maximum DC input voltage, V	374.8
Core type	EE32 (E32/6/20)
Core material	3F3
Nominal primary inductance, µH	210
Primary winding	14
Secondary main number of turns	3
Actual transformer fit factor, %	73.3
Frequency, kHz	90
Core cross-sectional area, mm^2	129
Maximum flux density, mT	320
Peak flux density, mT	344
Estimated gap length, mm	0.124
Estimated primary leakage inductance, µH	5.51

The schematic diagram of the planar transformer is shown in Figure 1a. The location of the coils in the core is shown in Figure 1b. The primary winding is arranged in four layers: E1:P1, E1:P2, E3:P1, and E3:P2 (red color). It has two double-sided foiled printed circuit boards with seven windings each; the secondary winding is located on a double-sided foiled printed circuit board (PCB) in layers E2:P6 and E2:P7 (blue color), with a total of three windings. In layers E1:P4 and E1:P5 (orange color), a bias coil is located on one double-sided PCB with two windings. Based on the design results, a 3D model of the planar transformer was developed in COMSOL Multiphysics software (ver. 6.0), shown in Figure 1c.



(**a**) (**b**) (**c**)

Figure 1. Schematic diagram, assembly diagram and 3D model of the planar transformer: (**a**) Schematic diagram of the planar transformer; (**b**) Location of the coils in the core; (**c**) 3D model of the planar transformer was developed in COMSOL Multiphysics software.

https://doi.org/10.3390/engproc2026150086

To describe the electromagnetic field created by the primary winding of the transformer and its propagation in space-time, a system of Maxwell's equations for the frequency domain is used [9]—Equation (1) is as follows:

$$\left| \begin{array}{l} \nabla \times H = J \\ B = \nabla \times A \\ J = \sigma E + j\omega D + J_e \\ E = -j\omega A \end{array} \right. \quad (1)$$

where ∇—del operator; H—magnetic field intensity; J—current density; B—magnetic flux density; A—magnetic vector potential; σ—conductivity; E—electric field intensity; j—imaginary part; ω—angular frequency; D—electric flux density; and J_e—externally generated current.

The boundary conditions used can be found in Equation (2):

$$n \times A = 0, \quad (2)$$

where n is the normal vector.

Electrostatic field equations (stationary problem) are used to calculate the self-capacitances of the coils—Equation (3) is as follows:

$$\left| \begin{array}{l} \nabla \times D = \rho_v \\ E = -\nabla V_e \end{array} \right. , \quad (3)$$

where ρ_v—volume charge density and V_e—electric vector potential.

The boundary conditions used can be found in Equation (4):

$$n \times D = 0, \quad (4)$$

The boundary conditions used are A = 0 in the electromagnetic problem, and D = 0 in the electrostatic problem.

The determination of the self-inductance of the primary winding L1 is carried out by means of the magnetic energy [9]—Equations (5) and (6) are as follows:

$$W_m = \int_V \left(\int_0^B H.dB \right).dV = \int_V \left(\int_0^T H.\frac{\partial B}{\partial t} dt \right).dV, \quad (5)$$

where V—volume; T—period; and t—time.

$$L_1 = \frac{2W_m}{I_L^2}, \quad (6)$$

where L_1—inductance of the primary coil and I_L—current in the primary coil.

The magnetizing inductance L_{mag} is determined using Equation (7) [1]:

$$L_{mag} = \frac{\mu_0 \mu_e N_{prim}^2 A_c}{l_c}, \quad (7)$$

where μ_0—vacuum magnetic permeability $\mu_0 = 4\pi \times 10^{-7}$ H/m; μ_e—effective permeability; N_{prim}—number of primary turns; A_c—cross-sectional area of the core; and l_c—the length of magnetic path in core.

https://doi.org/10.3390/engproc2026150086

The peak magnetizing current can be determined by Equation (8):

$$I_{mp} = \frac{B_m l_c}{\mu_0 \mu_e N_{prim}}, \quad (8)$$

where B_m—maximum flux density.

The leakage inductance L_{lk} of the transformer is related to energy storage in the magnetic field of the transformer. The leakage inductance can be expressed by Equation (9):

$$L_{lk} = \frac{\mu_0 N_{prim}^2 MLTb}{3w}, \quad (9)$$

where *MLT*—mean length of a turn, and b and w are the breadth and width of the winding.

The AC resistance RAC of the primary winding can be determined using Dowell's equation, accounting for skin effect and proximity effect—Equation (10):

$$R_{AC} = R_{DC}\Delta\left(\varepsilon_1 + \frac{2(p^2-1)}{3}\varepsilon_2\right), \quad (10)$$

where R_{DC}—DC resistance of the coil; $\Delta = \frac{t_t}{\delta}$; t_t—coil thickness; δ—skin depth; $\varepsilon_1 = \frac{\sinh 2\Delta + \sin 2\Delta}{\cosh 2\Delta - \cos 2\Delta}$; $\varepsilon_2 = \frac{\sinh 2\Delta - \sin 2\Delta}{\cosh 2\Delta + \cos 2\Delta}$; p—number of winding layers.

The stored electrical energy is used to determine the self-capacitance of the coils—see Equation (11):

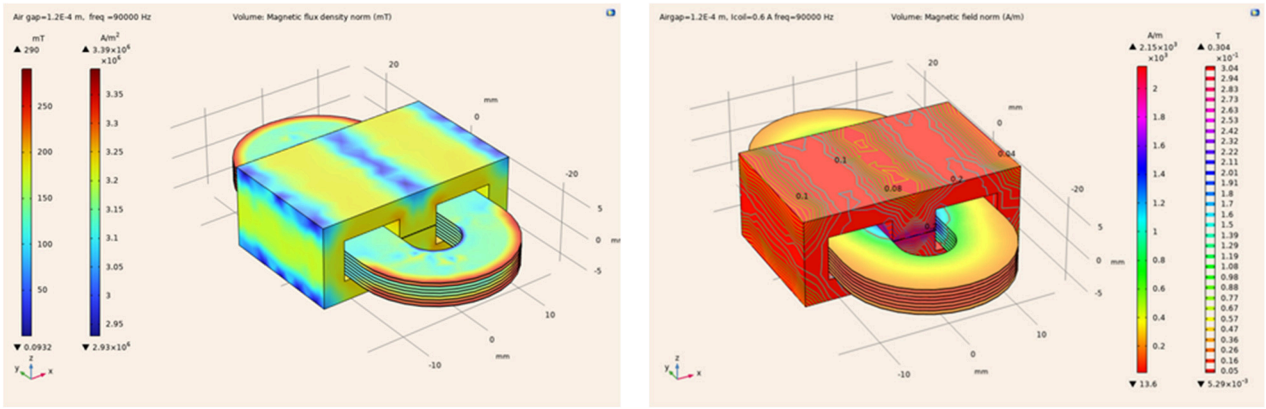
$$W_e = \int_V \left(\int_0^D E.dD\right).dV = \int_V \left(\int_0^T E.\frac{\partial D}{\partial t}dt\right).dV, \quad (11)$$

The model of the electromagnetic and electric field is obtained by means of the created geometric 3D model of a planar transformer at a fixed air gap value of 0.12 mm, operating frequency of 90 kHz, and effective value of the current in the primary winding of 0.6 A.

3. Results

3.1. Magnetic Flux Density, Magnetic Field Intensity, Electrical Potential and Electric Field Intensity

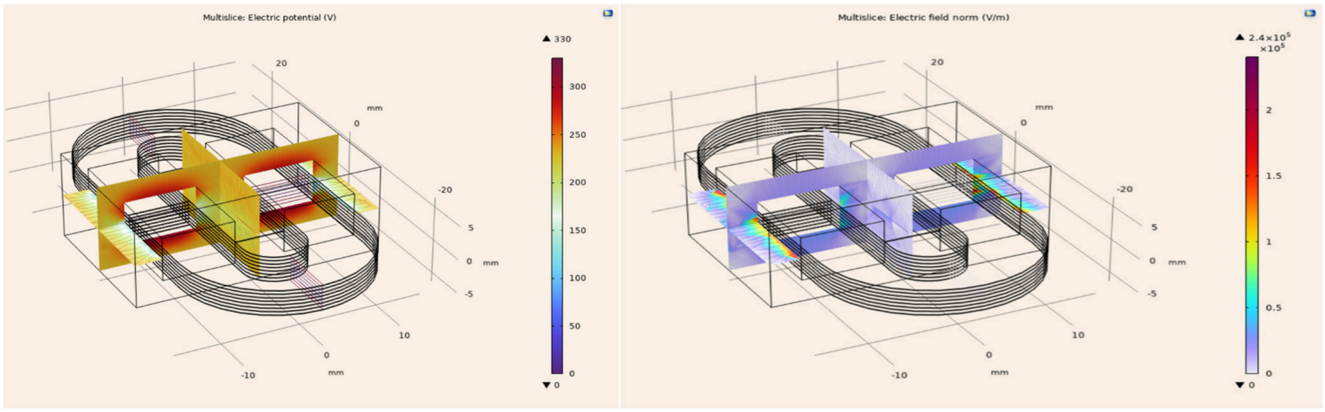
Figure 2 illustrates the results obtained from the electromagnetic field modeling of the planar transformer, performed with an air gap of 0.12 mm and an operating frequency of 90 kHz.



(**a**) (**b**)

Figure 2. Electromagnetic field modeling of the planar transformer: (**a**) normalized magnetic induction and normalized current density; (**b**) normalized magnetic field intensity and magnetic induction.

Figure 3 shows a distribution of the electric potential and electric field normalized.



(**a**) (**b**)

Figure 3. Distribution of the electric potential and electric field normalized of a planar transformer: (**a**) modeling the electric potential at an air gap of 0.12 mm, current in the primary winding of 0.6 A, and operating frequency of 90 kHz; (**b**) modeling the electric field at an air gap of 0.12 mm, current in the primary winding of 0.6 A and operating frequency of 90 kHz.

It can be seen from the figures that the maximum value of the magnetic flux density in the core is 0.304 T, which coincides with the previously calculated maximum flux density, shown in Table 1. The lines of the magnetic flux density and the distribution of the current density, a view of the electric potential and the electric field show the adequacy of the created model.

3.2. Dependence of the Inductance of the Primary Winding on the Air Gap

Figure 4 shows the dependence of the inductance of the primary winding on the air gap.

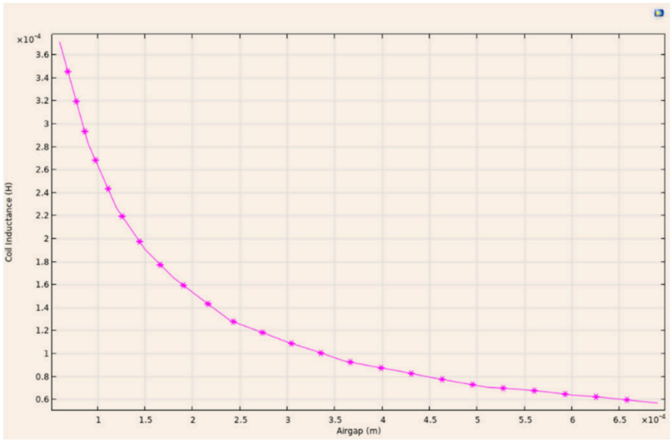


Figure 4. Dependence of the inductance of the primary winding on the air gap.

An increase in the air gap leads to a decrease in the effective magnetic permeability μ_e and an increase in the total magnetic resistance of the core, which is the sum of the magnetic resistances of the transformer's core and the air gap. As a result of the inversely proportional dependence of the inductance of the primary winding on the total magnetic resistance, it decreases with increasing air gap.

4. Model Verification

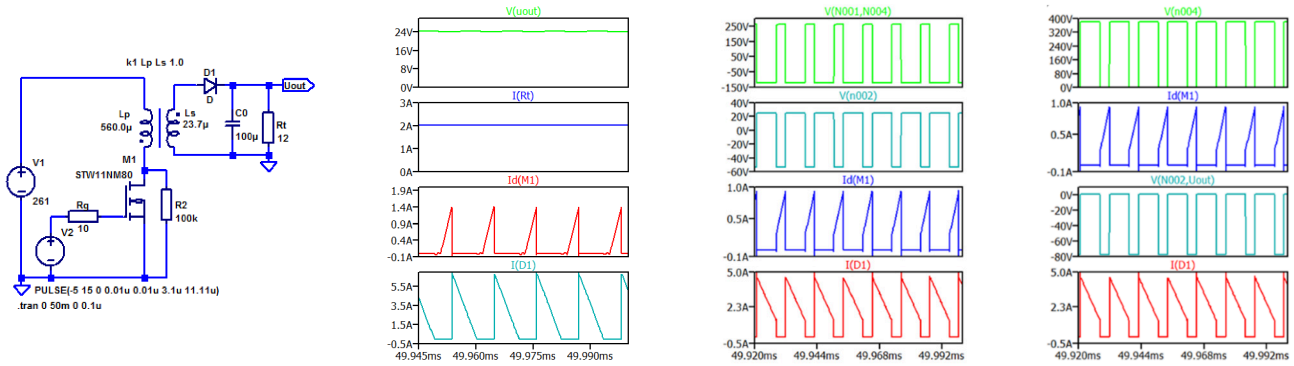
To verify the developed model and the obtained results, simulations of the operation of the flyback converter are carried out with the values of the equivalent parameters

calculated from the modeling, as shown in Table 2. Simulations of the operation of the flyback converter in two modes of operation, continuous current mode and border mode, have been done.

Table 2. Modeling results of a planar transformer.

Parameters	Value
Magnetizing inductance, (mH)	1.32
Primary coil resistance, (mΩ)	145
Primary leakage inductance, (µH)	5.47
Primary leakage resistance, (mΩ)	38.57
Primary coil self-capacitance, (pF)	41.13
Secondary coil self-capacitance, (pF)	746.23
Primary coil inductance, (µH)	219.75
Secondary coil inductance, (µH)	55.53

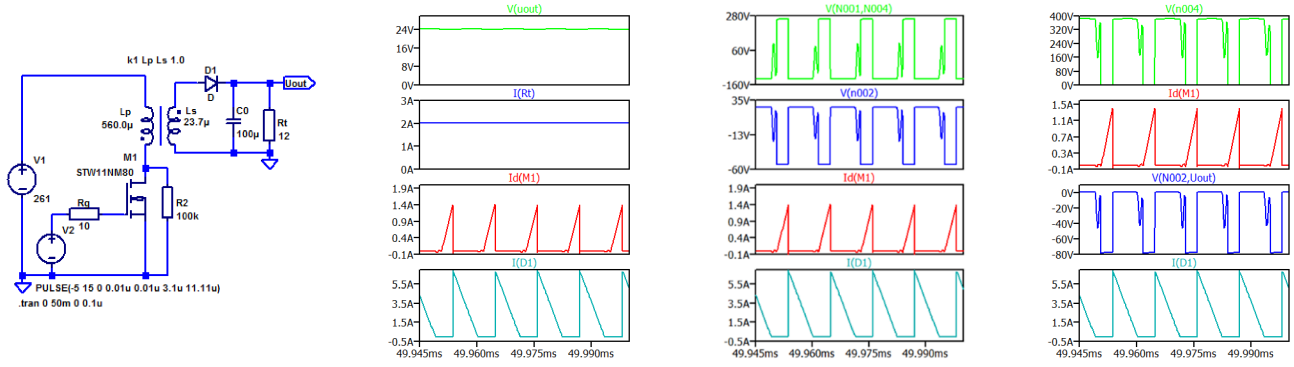
Figure 5 shows a simulation model of a flyback converter operating in continuous current mode.



(**a**) (**b**) (**c**) (**d**)

Figure 5. Simulation model of a flyback converter operating in continuous current mode: (**a**) circuit diagram; (**b**) output voltage, load current, transistor current, and diode current; (**c**) voltage across primary and secondary winding; (**d**) voltage across transistor and diode.

Figure 6 shows the operation of the converter in the border mode.



(**a**) (**b**) (**c**) (**d**)

Figure 6. Operation of the converter in the border mode: (**a**) circuit diagram; (**b**) output voltage, load current, transistor current, and diode current; (**c**) voltage across primary and secondary winding; (**d**) voltage across transistor and diode.

From the presented simulations of the flyback converter operation, using parameters obtained from the modeling, it can be observed that the calculated parameters of the planar

transformer ensure stable operation of the bridge converter, without voltage and current dips or disturbances.

The output current and output voltage correspond to the design values. Based on the calculated maximum values of current and voltage, the selection of components for the flyback converter circuit can be performed.

5. Conclusions

This paper presents a 3D model of a planar transformer for a flyback converter. An approach is proposed for determining the magnetizing inductance, leakage inductance, primary winding resistance, self-capacitances, and the inductances of the primary and secondary windings. The obtained results are verified through simulation of the flyback converter operation using LTSpice software (ver. XVII). The simulation results show that the converter operates stably, without voltage and current dips or disturbances. The output current and voltage of the flyback converter correspond to the design specifications. Future work will focus on developing a physical prototype of the planar transformer and the flyback converter, as well as on experimental validation of the results and further model refinement to optimize self-capacitances and leakage inductance.

Author Contributions: Conceptualization, H.I., D.A. and M.Y.; methodology, H.I., D.A. and M.Y.; software, H.I. and D.A.; validation, H.I., D.A. and M.Y.; formal analysis, D.A.; investigation, M.Y.; resources, M.Y.; data curation, H.I. and M.Y.; writing—original draft preparation, H.I., D.A. and M.Y.; writing—review and editing, H.I. and D.A.; visualization, H.I.; supervision, D.A.; project administration, H.I.; funding acquisition, M.Y. All authors have read and agreed to the published version of the manuscript.

Funding: This research was funded by the European Regional Development Fund within the OP "Research, Innovation and Digitalization Programme for Intelligent Transformation 2021–2027", Project No. BG16RFPR002-1.014-0005 Center of Competence "Smart Mechatronics, Eco- and Energy Saving Systems and Technologies".

Institutional Review Board Statement: Not applicable.

Informed Consent Statement: Not applicable.

Data Availability Statement: Data are available in this manuscript.

Conflicts of Interest: The authors declare no conflicts of interest.

Abbreviations

The following abbreviations are used in this manuscript:

3D	Three-Dimensional
DC	Direct Current
AC	Alternating Current
PCB	Printed Circuit Board
MLT	Mean Length of a Turn

References

1. Hurley, W.G.; Wölfle, W.H. *Transformers and Inductors for Power Electronics: Theory, Design and Applications*, 1st ed.; John Wiley & Sons Ltd.: Hoboken, NJ, USA, 2013; pp. 237–264, ISBN 978-1-119-95057-8.
2. Ibrishimov, H. Modeling planar transformer for DC/DC converter. In Proceedings of the International Scientific Conference (UNITECH 2020), Gabrovo, Bulgaria, 20–21 November 2020.
3. Djuric, S.; Stojanovic, G.; Damnjanovic, M.; Radovanovic, M.; Laboure, E. Design, modeling, and analysis of a compact planar transformer. *IEEE Trans. Magn.* **2012**, *48*, 4135–4138. [CrossRef]

4. Ouyang, Z.; Thomsen, O.C.; Andersen, M.A.E. Optimal design and tradeoff analysis of planar transformer in high-power DC–DC converters. *IEEE Trans. Magn.* **2012**, *57*, 2800–2810. [CrossRef]
5. Chandwani, A.; Mallik, A. Parametric modeling and characterization of leakage-integrated planar transformer for CLLC DC–DC converter. *IEEE Trans. Magn.* **2022**, *58*, 1–8. [CrossRef]
6. Margueron, X.; Keradec, J.-P.; Magot, D. Analytical calculation of static leakage inductances of HF transformers using PEEC formulas. *IEEE Trans. Ind. Appl.* **2007**, *43*, 884–892. [CrossRef]
7. Østergaard, C.; Kjeldsen, C.S.; Nymand, M. Calculation of planar transformer capacitance based on the applied terminal voltages. In Proceedings of the IEEE 21st Workshop on Control and Modeling for Power Electronics (COMPEL), New York, NY, USA, 9 November 2020.
8. Arnaudov, D.D.; Madzharov, N.D.; Hinov, N.L. Rotary Wireless Inductive Transmitter Powered by ZVS Resonant Convertor. *Elektron. ir Elektrotechnika* **2019**, *25*, 17–22. [CrossRef]
9. *COMSOL Multiphysics*, Version 6.0; COMSOL AB: Stockholm, Sweden, 2024.

Disclaimer/Publisher's Note: The statements, opinions and data contained in all publications are solely those of the individual author(s) and contributor(s) and not of MDPI and/or the editor(s). MDPI and/or the editor(s) disclaim responsibility for any injury to people or property resulting from any ideas, methods, instructions or products referred to in the content.